

## The Diagnosis of Lung Cancer Using 1064-nm Excited Near-infrared Multichannel Raman Spectroscopy

Hiroya Yamazaki,<sup>\*\*\*</sup> Shoji Kaminaka,<sup>\*\*\*</sup> Ehiichi Kohda,<sup>\*</sup> Makio Mukai,<sup>\*\*\*</sup>  
and Hiro-o Hamaguchi<sup>\*\*</sup>

**Purpose:** Raman spectroscopy is based on Raman scattering of light from molecules. Because the wavelength of Raman scattered light depends on molecular composition, Raman spectra provide highly useful information about molecular composition. It has already been shown that Raman spectroscopy is potentially useful for the clinical diagnosis of malignant tumors. However, this technique had never been applied to the diagnosis of lung cancers, primarily because of interference from the strong fluorescence emitted from lung tissues. Our purpose was to examine the effectiveness of near-infrared Raman spectroscopy for the diagnosis of lung cancers.

**Methods:** We constructed a new near-infrared multichannel Raman system that is capable of measuring high signal-to-noise ratio, fluorescence-free Raman spectra of lung tissues within a measurement time of 1 second. Using this system, we collected a total of 210 Raman spectra from cancerous and non-cancerous lung tissues and analyzed these spectra by a least-squares fitting procedure for cancer diagnosis.

**Results:** The resultant sensitivity of cancer prediction was as high as 91%, with 97% specificity and an error margin of  $p < 0.0001$  according to Fisher's exact test.

**Conclusions:** A method of diagnosing lung cancer efficiently and objectively using Raman spectroscopy has thus been established.

**Key words:** diagnosis, lung neoplasms, Raman spectroscopy

### INTRODUCTION

WITH DEVELOPMENTS in medical imaging technologies such as ultrasonography, computed tomography, and magnetic resonance imaging, there has been rapid progress in the clinical diagnosis of cancers. Nevertheless, there are still a number of occasions in which needle biopsy has to be chosen. Biopsy can be an invasive procedure and is inevitably associated with the risk of dissemination. Considerable time and cost are

required to obtain the biopsy sample, and the specialized knowledge of a pathologist is needed for diagnosis. In order to overcome these problems, various attempts have been made, such as those using tumor markers, to achieve minimally invasive clinical diagnoses of cancers. Recent attention in this regard has been directed toward the use of Raman spectroscopy, which is ideally suited for the minimally invasive diagnosis of cancer at the molecular level.<sup>1-9</sup>

Raman spectroscopy is based on Raman scattering, an inelastic scattering of light from molecules. When light is incident on a substance, a very small portion of the incident light is dispersed as Raman scattering. The wavelength of Raman-scattered light depends on the molecular composition of the substance. Therefore, Raman spectra, which are often called "molecular fingerprints", provide highly useful information about the composition of the substance at the molecular level. It has already been shown by several groups that Raman spectroscopy is potentially useful for the clinical

---

Received August 1, 2002; revision accepted November 29, 2002.

Department of <sup>\*</sup>Radiology and <sup>\*\*\*</sup>Pathology, Keio University School of Medicine

<sup>\*\*</sup>Department of Chemistry, School of Science, the University of Tokyo

Reprint requests to Hiroya Yamazaki, M.D., Department of Radiology, Keio University School of Medicine, 35 Shinanomachi, Shinjuku, Tokyo 160-8582, JAPAN.

This work was partially supported by Grants-in-Aid (No. 12354007 and 12877145) from the Ministry of Education, Science and Culture.

diagnosis of malignant tumors.<sup>1-9</sup>

However, a few experimental difficulties have hindered the practical application of Raman spectroscopy to diagnosis. First, the Raman scattering signal is very weak, necessitating an extremely sensitive method of detection such as photon counting. Second, human tissues are strongly fluorescent if excited by visible/ultraviolet light, and this fluorescence masks entirely the much weaker Raman scattering signals. Third, irradiation of strong visible/ultraviolet light may be hazardous to the human body. The second and third difficulties can be overcome if deep near-infrared light ( $\lambda > 1 \mu\text{m}$ ) is used for excitation. However, the detectors so far available in this wavelength region have been much less sensitive than those in the visible/ultraviolet region, thereby limiting the practicability of near-infrared Raman spectroscopy.

We recently constructed a near-infrared Raman spectroscopic system with much higher sensitivity than the previously reported systems, using a newly developed near-infrared multichannel detector with an Indium phosphide/Indium-Gallium-Arsenide phosphide (InP/InGaAsP) photocathode. This new detector achieves high sensitivity of up to 1400 nm, which is comparable with photon counting. By using the 1064-nm line of a Nd:YAG laser for excitation, we are able to eliminate fluorescence almost entirely from the Raman spectrum and minimize the effects of irradiation on the human body. Thus, the three difficulties mentioned above have been overcome by the present development of the new near-infrared multichannel Raman system.

The issue that remains is how clearly cancer can be diagnosed by Raman spectroscopy. As far as the authors are aware, the present paper is the first in which this issue is discussed on the basis of a statistical procedure using a number of (210) Raman spectra of the same human tissues (lung tissues) with and without cancers.

## MATERIALS AND METHODS

We used specimens of 35 lungs extracted during operations or obtained at autopsies. Of those specimens, 28 were from males and seven from females, with ages ranging from 44 to 88 years (average, 66 years). The histopathological diagnoses included 14 squamous cell carcinomas, 18 adenocarcinomas, one adenosquamous carcinoma, and two large cell carcinomas. None of the patients had had radiotherapy or chemotherapy before surgery. The lung specimens were preserved in 10% formaldehyde solution. A cube of 5 mm was cut from the cancerous portion of each lung, and Raman spectra were measured at three different positions for each sample. A total of 105 Raman spectra were thus obtained

from the cancerous samples. The same procedure was followed for the non-cancerous part of each lung, also giving a total of 105 Raman spectra of non-cancerous samples. All measurements were carried out under room light and at room temperature.

The Raman spectroscopic system we used is shown in Fig. 1. The 1064-nm line of a Nd:YAG laser (repetition rate 25 kHz, pulse width 100 ns, average power 120 mW at sample point) was used for excitation. The laser beam was focused into a 0.1 mm  $\times$  1 mm sample area by using two cylindrical lenses. The backscattered light from the sample was collected by a pair of lenses and focused on the entrance slit of a polychromator and detected by a newly developed near-infrared multichannel detector<sup>10</sup> with an InP/InGaAsP photocathode (Hamamatsu Photonics, Shizuoka, Japan, quantum efficiency  $\sim 1\%$ ). The detector was gated (100 ns gate width) in order to eliminate thermal noise and contamination by room light. Two holographic notch filters and a glass filter were used to eliminate elastic scattering and room light, respectively. Exposure time was 1 second. The spectrum was obtained 400 times, then averaging was performed at each sampling point. All measurements were made in the wavenumber range of 1315 to 1720  $\text{cm}^{-1}$ , and background was subtracted from each spectrum (Fig. 2). The background curve for each spectrum was determined by a least squares fitting of a quadratic function to three data points in the spectrum at 1367  $\text{cm}^{-1}$ , 1529  $\text{cm}^{-1}$ , and 1720  $\text{cm}^{-1}$ . These three points were selected because they are not affected by any Raman bands and therefore are suitable for estimating the baseline. After the experiment, each tissue sample was used to create a hematoxylin and eosin (HE) stained specimen, and tissue diagnosis was performed by a pathologist to establish the histopathological diagnosis of the sample.

In order to standardize the Raman spectra of cancerous and non-cancerous tissues, we averaged all the observed Raman spectra to obtain two standard spectra, one for cancerous tissues ( $S_c$ ) and one for non-cancerous tissues ( $S_{nc}$ ) (Fig. 3). Note that the two spectra are normalized so that total area intensities are the same. Each observed spectrum was then fitted by a least-squares calculation to a linear combination of the two standard spectra,

$$\text{Observed spectra} = a \times S_c + b \times S_{nc},$$

where  $a$  and  $b$  are positive coefficients. If the observed spectrum completely agrees with  $S_c$ ,  $b=0$ , while if it agrees with  $S_{nc}$ ,  $a=0$ . All the intermediate spectra have non-zero  $a$  and  $b$  coefficients. Here we use the ratio  $\chi = a/(a+b)$  as a diagnostic parameter. The parameter  $a/(a+b)$  tends to be close to 1 if the spectrum contains more

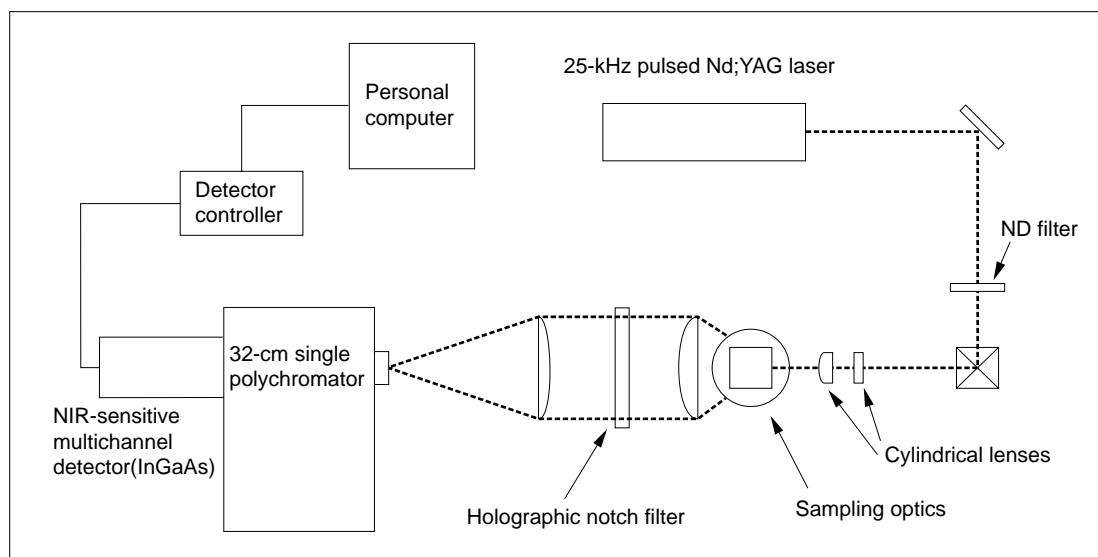


**Fig. 1.** Layout of the 1064-nm excited near-infrared multichannel Raman system.

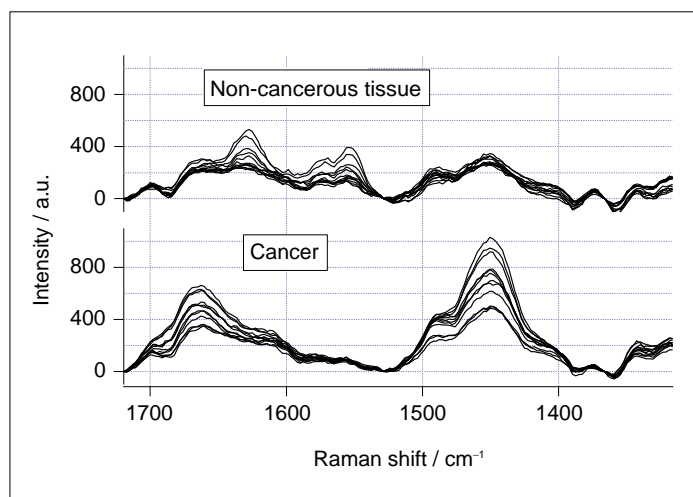


**Fig. 2.** Observed Raman spectra of cancerous and normal human lung tissues.

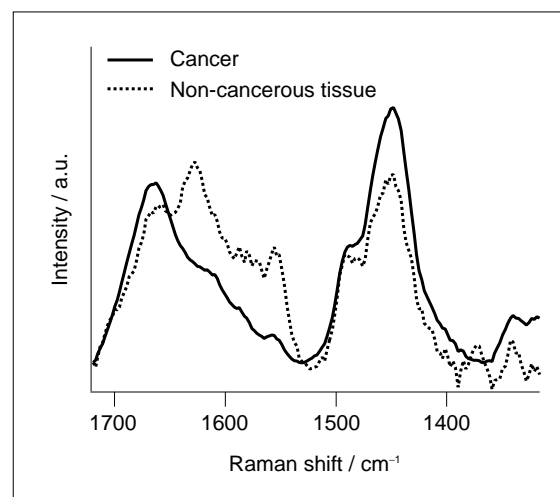


**Fig. 3.** Standard Raman spectra of cancerous and non-cancerous tissues.

characteristics of  $S_c$ , while it approaches 0 if the spectrum more closely resembles  $S_{nc}$ .

## RESULTS

### Characteristic peaks for cancerous and non-cancerous tissues

The observed Raman spectra of cancerous and non-cancerous tissues after background subtraction were compared (Fig. 2). Characteristic peaks were observed at  $1342\text{ cm}^{-1}$ ,  $1448\text{ cm}^{-1}$ ,  $1488\text{ cm}^{-1}$ ,  $1554\text{ cm}^{-1}$ , and  $1662\text{ cm}^{-1}$  for both cancerous and non-cancerous tissues. Another strong band was observed at  $1610\text{ cm}^{-1}$  for cancerous tissues and a shoulder at  $1627\text{ cm}^{-1}$  for non-

cancerous tissues. For cancerous tissues, the two bands at  $1448\text{ cm}^{-1}$  and at  $1662\text{ cm}^{-1}$  were much stronger than the others, while for non-cancerous tissues, the  $1554\text{ cm}^{-1}$  band was as strong as the  $1448\text{ cm}^{-1}$  band. The  $1448\text{ cm}^{-1}$  band is assigned to the  $\text{CH}_2$ - bending vibrations of lipids and/or proteins and the  $1662\text{ cm}^{-1}$  band to the amide I band of proteins.<sup>5,7-9</sup> The other weak bands were assignable to nucleic acids and other molecular species, but their detailed assignment will need further consideration.

No tissue damage from laser irradiation was observed in any of the cancerous or non-cancerous samples during pathological examination after the Raman

measurements.

### Histogram presentation

A histogram presentation of the parameter  $\chi$  for all the 210 observed Raman spectra is shown in Fig. 4. Cancer diagnosis by Raman spectroscopy would be meaningful if the cancerous samples showed a strong tendency to  $\chi=1$  and the non-cancerous samples were inclined to  $\chi=0$ . The histogram shows that, for 102 of the 105 points (97%) of the non-cancerous tissues,  $\chi$  is less than 0.5. The three points with  $\chi>0.5$  came from the same patient, and, with this exception, all the points with  $\chi>0.5$  were from cancerous tissues. All points with  $\chi<0.1$  came from non-cancerous tissues, with no cancerous tissues involved.

Among the 105 measuring points from the cancerous tissues, 12 had a coefficient between  $0.1<\chi<0.5$ , and these came from six patients. Among these six patients, three had all three points in this range of  $0.1<\chi<0.5$ . In each of the three false cases, marked proliferation of interstitial tissue was found. We consider that the nine false spectra obtained from the three patients corresponded to the mixture of cancerous and non-cancerous tissues in accordance with the histopathological findings.

## DISCUSSION

In previous studies,<sup>5-9,11-16</sup> Raman spectroscopy with laser power in the range of 40 to 500 mW was used with measurement times ranging from 10 seconds to 35 minutes. Low laser power and short measurement times were achieved only by visible excitation. For deep near-infrared excitation at 1064 nm, the present laser power of 120 mW and the measurement time of 1 second are the lowest. These have been achieved thanks to the newly developed near-infrared multichannel detector. The effect of laser irradiation on tissue has thus been minimized in the present study, using a low light dose and long wavelength for excitation. In fact, no tissue damage from laser irradiation was detected in any of the cancerous or normal tissue samples examined in the present study.

To discriminate cancerous tissues from non-cancerous tissues, we used a calculation that set the cut-off point at 0.5, which is the ratio  $\chi=a/(a+b)$ . We obtained a rate of sensitivity as high as 91% and a specificity of 97% for cancerous tissues. We consider these values very high compared with those in previous reports.<sup>4,5</sup> A margin of error of  $p<0.0001$  was obtained using Fisher's exact test. From these statistical data,  $\chi=0.5$  seems to be a good cut-off point. In our spectral analysis, we only subtracted the background and did not have to perform any of the

other mathematical procedures that were needed in previous research. Owing to this much simpler procedure, the measured spectra can be analyzed and diagnosed immediately on a computer.

Raman spectroscopy has been applied to the diagnosis of hepatocellular carcinoma,<sup>1</sup> uterine cervical cancer,<sup>3-6</sup> breast cancer,<sup>7,8</sup> and malignant skin lesions.<sup>9</sup> However, it had never been applied to the diagnosis of lung cancers, primarily because of interference from the strong fluorescence of unknown origin emitted from lung tissues if excited at shorter wavelengths. In the present study, by using the 1064-nm near-infrared laser line, we were able to avoid the effect of fluorescence and obtained high signal-to-noise ratio (S/N) Raman spectra of lung tissues, which had previously been thought impossible to measure. Furthermore, near-infrared laser excitation and gated detection made it possible to perform measurements under room light. Although the tissue samples we used were preserved in a 10% formaldehyde solution, the good correspondence between *in vitro* and *in vivo* measurements has already been established in previous research.<sup>6</sup> We believe results similar to those shown here will be obtained from measurements on live patients.

We were not able to differentiate normal tissue from inflammatory tissue in the wavenumber range of 1315 to 1720  $\text{cm}^{-1}$ . However, in the wavenumber range of 800 to 1800  $\text{cm}^{-1}$ , we have confirmed significant differences in near-infrared singlechannel Raman spectroscopy. Another defect of our study is that we could not examine benign lung nodular lesions such as old tuberculosis, sclerosing hemangioma, and so on, because they were not objects for operation. Even though this area remains to be researched, we at least were able to define the difference between normal and cancerous tissue.

We have also found a difference in spectra between squamous cell carcinoma and adenocarcinoma.<sup>17</sup> A typical Raman spectrum in the 1500 to 1700  $\text{cm}^{-1}$  wavenumber region of cancerous tissue is shown in Fig. 5. Using a curve-fitting analysis, we could decompose the observed spectra into five components, bands A to E. We made band A the intensity standard, and quantified the spectral difference by the relative intensity of (band B + band C) to band A. By using the cut-off point of 0.5, which is the relative intensity of (band B + band C) to band A, we distinctly separated the Raman spectra of adenocarcinoma and squamous cell carcinoma. Based on this evidence, we consider that the Raman spectra provide enough information to make the distinction not only between cancerous and non-cancerous tissues but also between cancerous tissues of different types.

In addition, we have succeeded in obtaining the

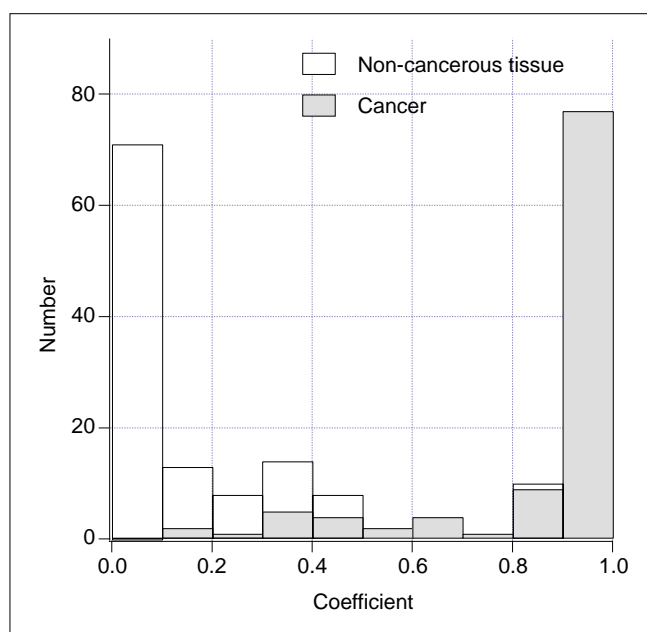


Fig. 4. Histogram representation of the distribution of the coefficient  $\chi = a/(a+b)$ .

spectra of metastatic lung cancers and have found a difference in spectra between primary and metastatic lung cancers (not published). Therefore, Raman spectroscopy will be established in the near future as a powerful new tool for real-time *in vivo* minimally invasive diagnosis of lung cancers.

Reliable lung cancer diagnosis has been shown to be possible by using the newly developed near-infrared multichannel Raman system. Raman spectroscopy provides an objective analytical method of examining the molecular composition of human tissues and is highly useful in histopathological diagnosis. The system we developed is safe for use on live patients and can be used *in vivo*. In addition, we have succeeded in developing a fiberoptic Raman spectroscopic system<sup>17</sup> and have collected data from human skin. Therefore, our system may replace biopsy as a new minimally invasive method of diagnosing lung cancers.

#### ACKNOWLEDGMENTS

We wish to acknowledge Professor Atsushi Kubo and Professor Sachio Kuribayashi for their guidance throughout our research. We acknowledge the

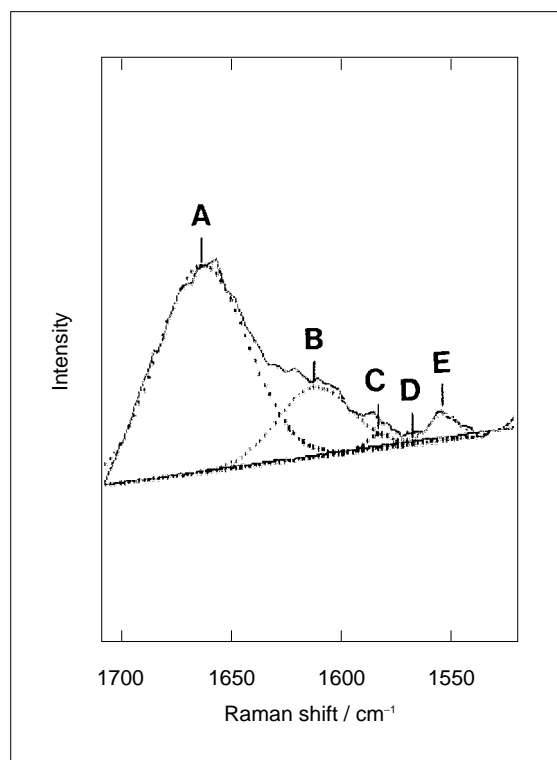


Fig. 5. Representative Raman spectrum of cancerous tissue and its curve-fitting decomposition. The spectrum is resolved into five components, bands A to E.

contributions of Professor Koichi Kobayashi and Professor Toshiharu Ishii to the clinical and histopathological studies. We also acknowledge the contributions of Hirotsugu Hiramatsu and Nobuyuki Shiraga to the data analysis.

#### REFERENCES

- 1) Hawi SR, Campbell WB, Kajdacsy-Balla A, Murphy R, Adar F, Nithipatikom K. Characterization of normal and malignant human hepatocytes by Raman microspectroscopy. *Cancer Lett*, 110: 35–40, 1996.
- 2) Schut TCB, Puppels GJ, Kraan YM, Greve J, van der Maas LLJ, Figdor CG. Intracellular carotenoid levels measured by Raman microspectroscopy: comparison of lymphocytes from lung cancer patients and healthy individuals. *Int J Cancer*, 74: 20–25, 1997.
- 3) Cohenford MA, Rigas B. Cytologically normal cells from neoplastic cervical samples display extensive structural abnormalities on IR spectroscopy: implications for tumor biology. *Proc Natl Acad Sci U S A*, 95: 15327–15332, 1998.
- 4) Ramanujam N, Mitchell MF, Mahadevan A, *et al.* *In vivo* diagnosis of cervical intraepithelial neoplasia using 337-nm-excited laser-induced fluorescence. *Proc Natl Acad*

- Sci U S A*, 91: 10193–10197, 1994.
- 5) Mahadevan-Jansen A, Mitchell MF, Ramanujam N, *et al.* Near-infrared Raman spectroscopy for *in vitro* detection of cervical precancers. *Photochem Photobiol*, 68: 123–132, 1998.
  - 6) Mahadevan-Jansen A, Mitchell MF, Ramanujam N, Utzinger U, Richards-Kortum R. Development of a fiber optic probe to measure NIR Raman spectra of cervical tissue *in vivo*. *Photochem Photobiol*, 68: 427–431, 1998.
  - 7) Frank CJ, Redd DCB, Gansler TS, McCreery RL. Characterization of human breast biopsy specimens with near-IR Raman spectroscopy. *Anal Chem*, 66: 319–326, 1994.
  - 8) Frank CJ, McCreery RL, Redd DCB. Raman spectroscopy of normal and diseased human breast tissues. *Anal Chem*, 67: 777–783, 1995.
  - 9) Gniadecka M, Wulf HC, Nielsen OF, Christensen DH, Hercogova J. Distinctive molecular abnormalities in benign and malignant skin lesions: studies by Raman spectroscopy. *Photochem Photobiol*, 66: 418–423, 1997.
  - 10) Kaminaka S, Yamazaki H, Ito T, Kohda E, Hamaguchi H. Near-infrared Raman spectroscopy of human lung tissue: possibility of molecular-level cancer diagnosis. *J Raman Spectroscopy*, 32: 139–141, 2001.
  - 11) Salenius JP, Brennan III JF, Miller A, *et al.* Biochemical composition of human peripheral arteries examined with near-infrared Raman spectroscopy. *J Vasc Surg*, 27: 710–719, 1998.
  - 12) Baraga JJ, Feld MS, Rava RP. *In situ* optical histochemistry of human artery using near infrared Fourier transform Raman spectroscopy. *Proc Natl Acad Sci U S A*, 89: 3473–3477, 1992.
  - 13) Brennan III JF, Romer TJ, Lees RS, Tercyak AM, Kramer Jr JR, Feld MS. Determination of human coronary artery composition by Raman spectroscopy. *Circulation*, 96: 99–105, 1997.
  - 14) Romer TJ, Brennan III JF, Fitzmaurice M, *et al.* Histopathology of human coronary atherosclerosis by quantifying its chemical composition with Raman spectroscopy. *Circulation*, 97: 878–885, 1998.
  - 15) Romer TJ, Brennan III JF, Schut TCB, *et al.* Raman spectroscopy for quantifying cholesterol in intact coronary artery wall. *Atherosclerosis*, 141: 117–124, 1998.
  - 16) Romer TJ, Brennan III JF, Puppels GJ, *et al.* Intravascular ultrasound combined with Raman spectroscopy to localize and quantify cholesterol and calcium salts in atherosclerotic coronary arteries. *Arterioscler Thromb Vasc Biol*, 20: 478–483, 2000.
  - 17) Kaminaka S, Ito T, Yamazaki H, Kohda E, Hamaguchi H. Near-infrared multichannel Raman spectroscopy toward real-time *in vivo* cancer diagnosis. *J Raman Spectroscopy*, 33: 498–502, 2002.